

## Evaluation of Anti-Alzheimer Activity of Synthetic Coumarins by Combination of *in Vitro* and *in Silico* Approaches

Ilkay Erdogan Orhan,<sup>a</sup> F. Sezer Senol Deniz,<sup>a</sup> Ramin Ekhteiri Salmas,<sup>b</sup> Sule Irmak,<sup>c</sup> Ozden Ozgun Acar,<sup>d</sup> Gurbet Celik Turgut,<sup>e</sup> Alaattin Sen,<sup>c, f</sup> Ana-Maria Zbancioc,<sup>g</sup> Simon Vlad Luca,<sup>h</sup> Adrianna Skiba,<sup>i</sup> Krystyna Skalicka-Woźniak,<sup>\*i</sup> and Gabriela Tatarina<sup>g</sup>

<sup>a</sup> Department of Pharmacognosy, Faculty of Pharmacy, Gazi University, 06330 Ankara, Turkey

<sup>b</sup> Department of Chemistry, Britannia House, King's College London, SE1 1DB London, UK

<sup>c</sup> Pamukkale University, Faculty of Arts & Sciences, Department of Biology, 20070 Denizli, Turkey

<sup>d</sup> Pamukkale University, Seed Breeding & Genetics Application Research Center, 20070 Denizli, Turkey

<sup>e</sup> Pamukkale University, Faculty of Applied Sciences, Organic Agriculture Management, Civril, 20680 Denizli, Turkey

<sup>f</sup> Abdullah Gul University, Faculty of Life and Natural Sciences, Department of Molecular Biology and Genetics, 38080 Kayseri, Turkey

<sup>g</sup> University of Medicine and Pharmacy Grigore T. Popa Iasi, Faculty of Pharmacy, Romania

<sup>h</sup> Biothermodynamics, TUM School of Life Sciences, Technical University of Munich, 85354 Freising, Germany

<sup>i</sup> Department of Natural Products Chemistry, Medical University of Lublin, 20-093 Lublin, Poland,, e-mail: kskalicka@pharmacognosy.org

Series of synthetic coumarin derivatives (**1-16**) were tested against acetylcholinesterase (AChE) and butyrylcholinesterase (BChE), two enzymes linked to the pathology of Alzheimer's disease (AD). Compound **16** was the most active AChE inhibitor with  $IC_{50}$   $32.23 \pm 2.91$   $\mu$ M, while the reference (galantamine) had  $IC_{50} = 1.85 \pm 0.12$   $\mu$ M. Compounds **9** ( $IC_{50}$   $75.14 \pm 1.82$   $\mu$ M), **13** ( $IC_{50} = 16.14 \pm 0.43$   $\mu$ M), were determined to be stronger BChE inhibitors than the reference galantamine ( $IC_{50} = 93.53 \pm 2.23$   $\mu$ M). The  $IC_{50}$  value of compound **16** for BChE inhibition ( $IC_{50} = 126.56 \pm 11.96$   $\mu$ M) was slightly higher than galantamine. The atomic interactions between the ligands and the key amino acids inside the binding cavities were simulated to determine their ligand-binding positions and free energies. The three inhibitory coumarins (**9**, **13**, **16**) were next tested for their effects on the genes associated with AD using human neuroblastoma (SH-SY5Y) cell lines. Our data indicate that they could be considered for further evaluation as new anti-Alzheimer drug candidates.

**Keywords:** Alzheimer's disease, cholinesterase inhibition, coumarin, molecular modeling, SH-SY5Y, biological activity, synthetic methods.

### Introduction

Alzheimer's disease (AD), the most common type of dementia, is a neurological disorder with progressive and irreversible character that mainly affects the elderly population over 60-year-old. AD is ranked as the 6<sup>th</sup> leading cause of death in the United States (US). On the other hand, the US Alzheimer's Association estimates that the incidence of AD would increase up to 13.8 million by 2060 country.<sup>[1]</sup> AD patients gradually experience memory loss, language prob-

lems, thinking and behavioral disabilities, seriously worsening their daily life.<sup>[2,3]</sup> At the moment, only symptomatic treatment is available. The current drugs are mostly cholinesterase (ChE) inhibitors and *N*-methyl-D-aspartate (NMDA) receptor antagonists, e.g., memantine. ChE family consists of two sister enzymes, e.g., acetylcholinesterase (AChE, EC 3.1.1.7) and butyrylcholinesterase (BChE, EC 3.1.18). Since acetylcholine (ACh) deficiency has been confirmed in the brains of AD patients, inhibition of AChE, the enzyme that

hydrolyzes ACh, is considered one of the main important treatment strategies against AD.<sup>[4]</sup> On the other hand, excess amounts of BChE and BChE-associated amyloid plaque formation has been described in AD pathology.<sup>[5]</sup> Thus, BChE inhibition has also become another therapeutic target for AD. Surely, other mechanisms, such as oxidative stress, mitochondrial dysfunction, and metal accumulation are involved in the complex pathology of AD.<sup>[6,7]</sup>

The current ChE inhibitory drugs, such as rivastigmine, tacrine, donepezil, and galantamine, have numerous side effects.<sup>[8]</sup> Consequently, extensive research to find novel ChE inhibitors with fewer side effects and enhanced efficiency is needed. For instance, many coumarin derivatives have been reported to possess promising inhibitory activity<sup>[9,10]</sup> and the ability of the 2H-chromen-2-one core to fit the enzymatic site have been proved.<sup>[11,12]</sup> Previously, series of natural coumarins (imperatorin, xanthotoxin, bergapten, pteryxin, hyuganin C, etc.) along with semisynthetic alkylated derivatives with encouraging inhibition against both ChEs enzymes have been investigated by our collaborative group.<sup>[13–16]</sup> In the light of this evidence, the aim of this study was to investigate ChE inhibitory activity of synthetic coumarin derivatives that were obtained in previous research (**1–16**, Table 1)<sup>[17]</sup> through a combinatorial approach using microtiter plate assays, cell culture experiments via SH-SY5Y cell lines, and molecular docking simulations.

## Results and Discussion

### ChE Inhibitory Activity of the Coumarins (1–16)

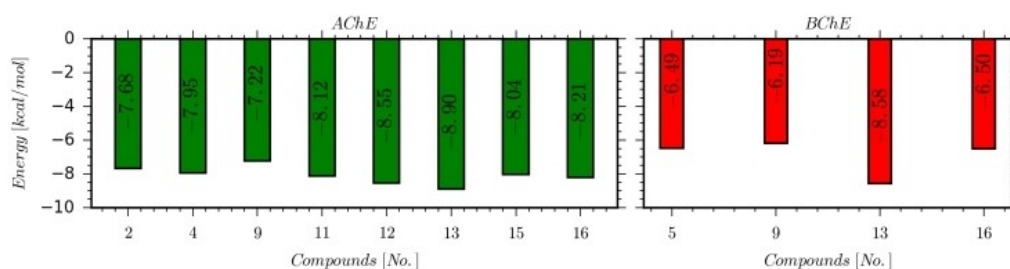
Previously synthesized novel coumarin derivatives (**1–16**) were screened for their ChE inhibitory activity. Results indicated that all of them were able to inhibit both ChEs at varying levels as tabulated in Table 2. Among them, coumarin derivatives **2**, **4**, **9**, **11**, **12**, **13**,

**15**, and **16** had AChE inhibition over 50% at 100 µg/mL. As indicated by their IC<sub>50</sub> values, the highest inhibition against AChE was produced by compound **16** (IC<sub>50</sub> = 32.23 ± 2.91 µM). In comparison the IC<sub>50</sub> value of galantamine was 1.85 ± 0.12 µM). On the other hand, compounds **5**, **9**, **13**, and **16** could also inhibit BChE, while compounds **5** and **16** had a higher IC<sub>50</sub> value (IC<sub>50</sub> = 195.04 ± 3.15 µM and IC<sub>50</sub> = 126.56 ± 11.96 µM) than that of galantamine (IC<sub>50</sub> = 93.53 ± 2.23 µM). These findings revealed that 7-hydroxy-4-propyl-coumarin (**9**), methyl 2-[2-((4-propyl-2-oxo-2H-chromen-7yl)oxy)acetyl]hydrazine-1-carbodithioate (**13**), and 7-ethoxy-4-propyl-2H-chromen-2-one (**16**) could promisingly block both of ChEs. The selectivity index (SI) of these three compounds were 0.31, 0.43, and 3.93, respectively.

### Molecular Docking Simulation of the Coumarins (1–16)

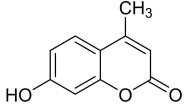
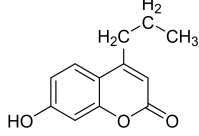
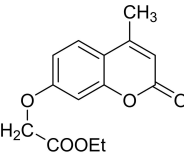
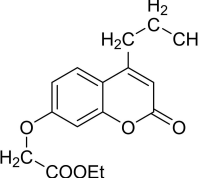
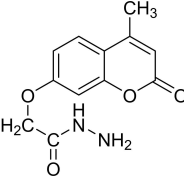
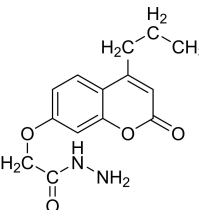
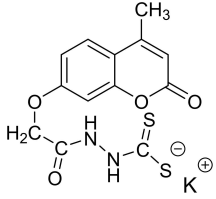
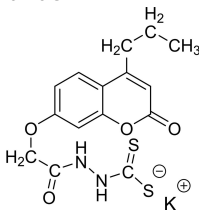
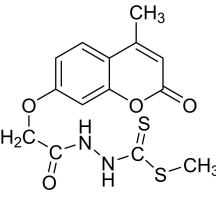
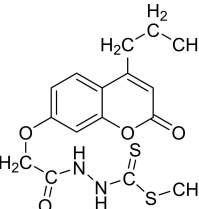
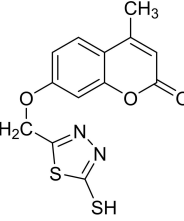
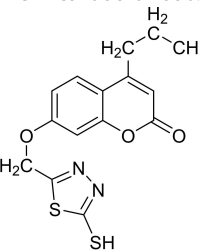
To have a better insight into the molecular mechanism of action, the ligand-protein interactions were simulated and the binding energies of all tested compounds inside AChE and BChE were estimated using docking simulations. All the docking scores fell into an acceptable range of binding energies and the compounds were therefore stable enough to bind strongly to the cavities as shown in Figure 1.

2D ligand-protein diagrams were reported in Figure 2, in which the active-site amino acids forming polar and nonpolar interactions with the ligands were shown. Amino acids around the ligands were classified by different colors according to their polarizability. Hydrogen bonds, π-π stacking, and salt bridges were among the most important interactions between the ligands and the binding domains. Both compounds **9** and **16** were firmly stabilized inside AChE by π-π stacking interactions and a hydrogen bond through Trp286 and Phe296, respectively. In addition to these amino acids, other neighboring hydrophobic amino acids also contributed to the interactions and shaped

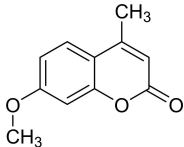
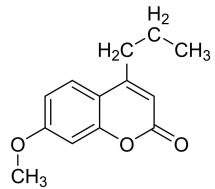
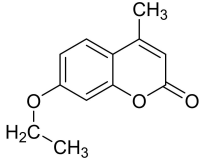
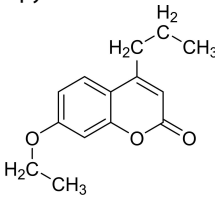


**Figure 1.** Docking scores of the active compounds inside the binding cavities of AChE and BChE targets.

**Table 1.** Chemical structures of the coumarin derivatives (1-16).

Compound	Structure	Compound	Structure
1	 <p>7-Hydroxy-4-methyl-2<i>H</i>-chromen-2-one</p>	9	 <p>7-Hydroxy-4-propyl-2<i>H</i>-chromen-2-one</p>
2	 <p>Ethyl 2-((4-methyl-2-oxo-2<i>H</i>-chromen-7-yl)oxy)acetate</p>	10	 <p>Ethyl 2-((4-propyl-2-oxo-2<i>H</i>-chromen-7-yl)oxy)acetate</p>
3	 <p>2-((4-Methyl-2-oxo-2<i>H</i>-chromen-7-yl)oxy)acetohydrazide</p>	11	 <p>2-((4-Propyl-2-oxo-2<i>H</i>-chromen-7-yl)oxy)acetohydrazide</p>
4	 <p>Potassium 2-(2-((4-methyl-2-oxo-2<i>H</i>-chromen-7-yl)oxy)acetyl)hydrazine-1-carbodithioate</p>	12	 <p>Potassium 2-(2-((4-propyl-2-oxo-2<i>H</i>-chromen-7-yl)oxy)acetyl)hydrazine-1-carbodithioate</p>
5	 <p>Methyl 2-(2-((4-methyl-2-oxo-2<i>H</i>-chromen-7-yl)oxy)acetyl)hydrazine-1-carbodithioate</p>	13	 <p>Methyl 2-(2-((4-propyl-2-oxo-2<i>H</i>-chromen-7-yl)oxy)acetyl)hydrazine-1-carbodithioate</p>
6	 <p>7-((5-Mercapto-1,3,4-thiadiazol-2-yl)methoxy)-4-methyl-2<i>H</i>-chromen-2-one</p>	14	 <p>7-((5-Mercapto-1,2,4-thiadiazol-2-yl)methoxy)-4-propyl-2<i>H</i>-chromen-2-one</p>

**Table 1.** (cont.)

Compound Structure	Compound Structure
<p><b>7</b></p>  <p>7-Methoxy-4-methyl-2H-chromen-2-one</p>	<p><b>15</b></p>  <p>7-Methoxy-4-propyl-2H-chromen-2-one</p>
<p><b>8</b></p>  <p>7-Ethoxy-4-methyl-2H-chromen-2-one</p>	<p><b>16</b></p>  <p>7-Ethoxy-4-propyl-2H-chromen-2-one</p>

**Table 2.** ChE inhibitory activity (inhibition % and IC<sub>50</sub> values) of the coumarins (**1-16**).

Compound	Enzyme Inhibition (Inhibition % ± S.D. <sup>a</sup> ) at 100 µg/mL <sup>b</sup> and IC <sub>50</sub> values AChE	BChE	Selectivity index (SI)
<b>1</b>	32.18 ± 0.86	40.65 ± 3.15	§ <sup>c</sup>
<b>2</b>	50.11 ± 1.89 (IC <sub>50</sub> = 532.10 ± 21.67 µM)	22.26 ± 3.26	§
<b>3</b>	47.88 ± 1.88	17.01 ± 0.45	§
<b>4</b>	54.97 ± 4.02 (IC <sub>50</sub> = 247.33 ± 12.06 µM)	7.48 ± 1.75	§
<b>5</b>	26.47 ± 1.60	61.06 ± 0.27 (IC <sub>50</sub> = 195.04 ± 3.15 µM)	§
<b>6</b>	46.85 ± 1.31	23.73 ± 1.02	§
<b>7</b>	43.41 ± 0.48	11.97 ± 0.15	§
<b>8</b>	34.18 ± 2.99	39.66 ± 2.54	§
<b>9</b>	66.49 ± 0.64 (IC <sub>50</sub> = 239.70 ± 11.84 µM)	93.09 ± 0.76 (IC <sub>50</sub> = 75.14 ± 1.82 µM)	0.31
<b>10</b>	13.06 ± 0.39	7.05 ± 0.95	§
<b>11</b>	62.68 ± 0.76 (IC <sub>50</sub> = 109.91 ± 1.56 µM)	12.50 ± 2.33	§
<b>12</b>	70.90 ± 1.88 (IC <sub>50</sub> = 91.62 ± 7.69 µM)	16.48 ± 2.63	§
<b>13</b>	79.41 ± 1.27 (IC <sub>50</sub> = 37.47 ± 0.87 µM)	98.77 ± 0.16 (IC <sub>50</sub> = 16.14 ± 0.43 µM)	0.43
<b>14</b>	43.65 ± 2.71	9.01 ± 2.32	§
<b>15</b>	81.01 ± 1.68 (IC <sub>50</sub> = 53.09 ± 3.77 µM)	38.35 ± 1.59	§
<b>16</b>	73.01 ± 0.57 (IC <sub>50</sub> = 32.23 ± 2.91 µM)	53.82 ± 1.32 (IC <sub>50</sub> = 126.56 ± 11.96 µM)	3.93
Reference <sup>d</sup>	97.11 ± 1.26 (IC <sub>50</sub> = 1.85 ± 0.12 µM)	77.94 ± 1.02 (IC <sub>50</sub> = 93.53 ± 2.23 µM)	50.68

<sup>a</sup> Standard deviation (n = 3). <sup>b</sup> Final concentration, <sup>c</sup> Not applicable. <sup>d</sup> Galantamine hydrobromide (100 µg/mL).

the binding cavity with the best possible positions for the ligand to form strong interactions. The 2D binding positions of the compounds **9** and **13** bound to the

active site of BChE were shown in *Figure 2*. The results demonstrated that BChE was able to properly accommodate both bulky and extended ligands. Pro285 and

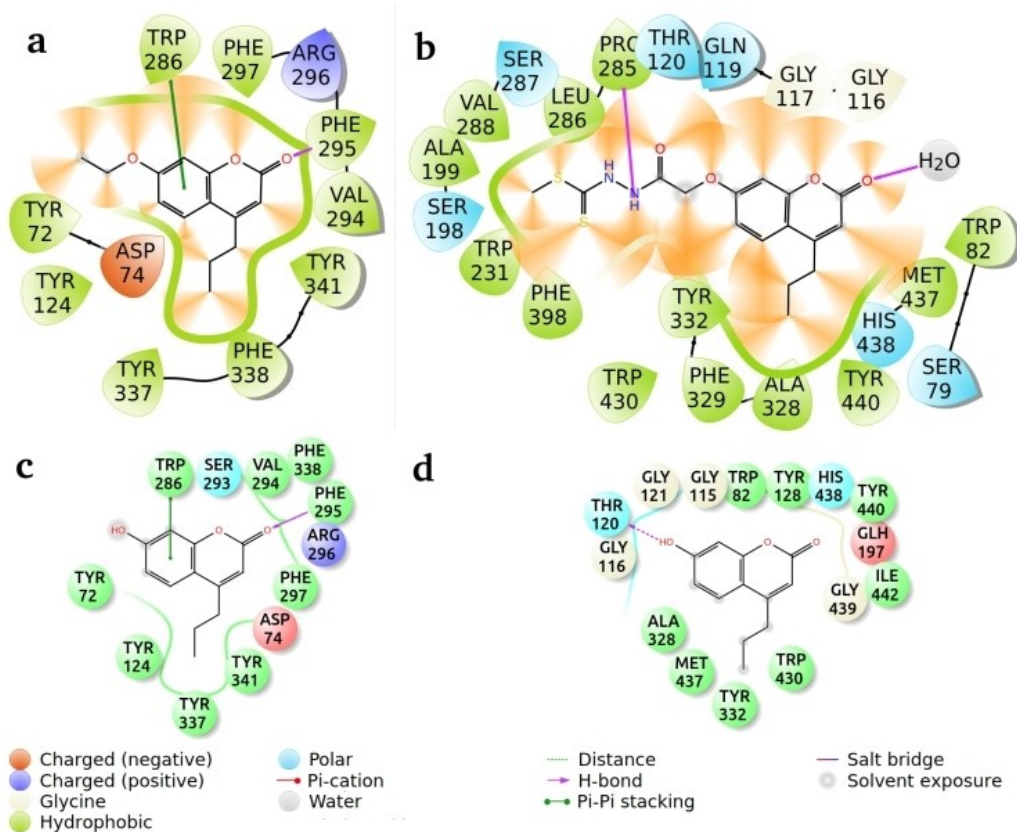


**Figure 2.** 2-D schematic views of the complexes 16-AchE (a), 13-BChE (b), 9-AChE (c) and 9-BChE (d), which are considered as the most stable ones. The active site amino acids within 4 Å of the ligands forming polar and non-polar interactions were shown in the diagrams.

Thr120 established a tight salt bridge and a hydrogen bond with the polar domains of the ligands. The critical role of a water molecule inside the binding domain forming a salt bridge with the oxygen atom linked to the ring domain is shown in *Figure 2*.

Based on the simulated interactions, the ring and the extended segments of the ligands are suggested

to play an effective role in stabilizing the inhibitors inside both AChE and BChE cavities. In addition to the 2D diagrams, the 3D positions of the compounds **13** and **16** inside AChE and BChE were rendered to show the 3D angles of the amino acids and the ligands with respect to each other, as shown in *Figure 3*.

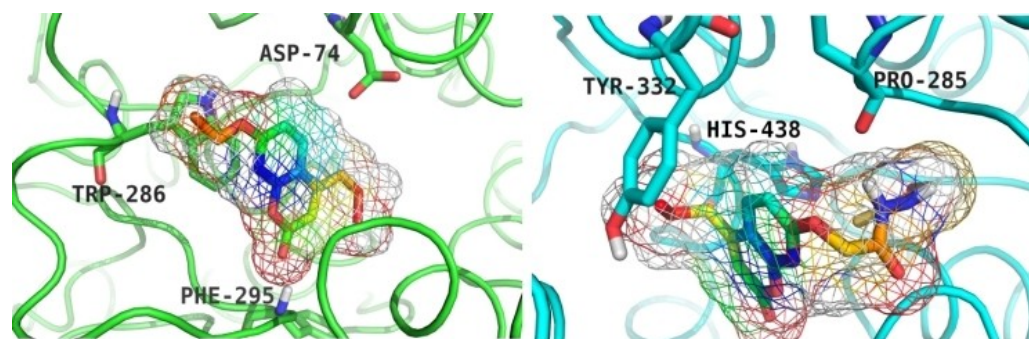


**Figure 3.** 3-D schematic views of the compounds **16** and **13** inside the active sites of the AChE and BChE targets. The diagrams show the docking positions of the ligands and the key active site amino acids around the ligands in 3-D forms.

### Effect of the Coumarins on SH-SY5Y Cells

In order to investigate the effects of the three active coumarin derivatives (**9**, **13**, and **16**) on the genes associated with AD and discover molecules that may have more potent effects than the current drugs used in AD treatment, further experiments were performed. For this purpose, the non-toxic concentrations of these compounds on SH-SY5Y cells, widely used in AD studies, were determined. The EC<sub>04</sub> and EC<sub>08</sub> values of the coumarin derivatives were determined by the crystal staining method.

As tabulated in Table 3, EC<sub>04</sub> and EC<sub>08</sub> values for **9**, **13**, and **16** were calculated as 0.80 μM and 1.05 μM, 0.45 μM and 0.75 μM as well as 3.28 μM, and 4.75 μM, respectively. When the cytotoxicity of these compounds on SH-SY5Y cells was compared, it was observed that **13** is almost 4- and 7- times more toxic than **9** and **16**, respectively.

The expression level of nine genes changed significantly after the treatment of the cells with the EC<sub>04</sub> of the compound **16**. A statistically significant

change was observed in the expression level of five genes after the treatment with EC<sub>08</sub> of the compound **16**. In addition, no significant change was observed in the expression levels of the studied genes at the EC<sub>04</sub> of compound **9**, while a statistically significant change was observed in the expression level of 6 genes after the treatment with EC<sub>08</sub> of compound **9** (Table 4). Thus, considering the AD treatment, compound **16** was more effective at low concentrations, as opposed to compound **9**, which was more effective at the higher concentration. This could be considered as an advantage for compound **16**, since it could exert desired actions without adverse effects due to the possible use of low concentrations. AD is the most common neurological disorder globally, and the increasing course of the disease continues.<sup>[18]</sup> Since the currently available agents cannot provide an efficient treatment, it is essential to search for new drugs that can be used to treat AD. Coumarin derivatives are remarkable bioactive compounds, with recent studies proving their anti-cancer, anti-HIV, anti-inflammatory, antibacterial, and anticoagulant activities.<sup>[19–22]</sup> In addition, numerous coumarins have been reported to have neuroprotective effects,<sup>[10,13]</sup> with several of them exerting anti-Alzheimer potential via inhibition of AChE activity.<sup>[9,13–15]</sup> Screening of the synthesized coumarin derivatives (**1–16**) indicated that all of them were able to inhibit both ChEs at different levels. There seems to be no direct relation between the structure of the tested coumarins and their

**Table 3.** EC<sub>04</sub> and EC<sub>08</sub> values of the coumarins **9**, **13**, and **16** in SH-SY5Y cells.

Tested coumarins	EC <sub>04</sub> (μM)	EC <sub>08</sub> (μM)
<b>9</b>	0.80	1.05
<b>13</b>	0.45	0.75
<b>16</b>	3.28	4.75

**Table 4.** The expression level of the selected genes in the SH-SY5Y cell lines<sup>a</sup>.

Genes	GenBank	<b>16</b> (EC <sub>04</sub> )	<b>16</b> (EC <sub>08</sub> )	<b>13</b> (EC <sub>04</sub> )	<b>13</b> (EC <sub>08</sub> )	<b>9</b> (EC <sub>04</sub> )	<b>9</b> (EC <sub>08</sub> )
<b>Beta-Amyloid Related</b>							
<b>APP</b>	NM_007471	<b>−2.81 ± 0.21<sup>b</sup></b>	1.94 ± 0.09	1.07 ± 0.26	−1.22 ± 0.13	1.36 ± 0.29	−1.22 ± 0.20
<b>PSEN1</b>	NM_000021	<b>−7.62 ± 0.56</b>	1.05 ± 0.12	1.25 ± 0.21	−1.59 ± 0.28	1.55 ± 0.09	<b>−3.07 ± 0.06</b>
<b>Lipid Metabolism</b>							
<b>ABCA7</b>	NM_019112	<b>−4.72 ± 0.52</b>	<b>3.08 ± 0.43</b>	1.13 ± 0.18	1.30 ± 0.26	1.32 ± 0.16	−1.53 ± 0.09
<b>APOE</b>	NM_000041	<b>−6.13 ± 0.61</b>	1.14 ± 0.19	1.12 ± 0.21	−1.29 ± 0.18	−1.41 ± 0.35	<b>−3.61 ± 0.26</b>
<b>CLU</b>	NM_001831	<b>−6.33 ± 0.89</b>	<b>−3.89 ± 0.37</b>	−1.75 ± 0.21	1.35 ± 0.27	1.20 ± 0.26	<b>−2.89 ± 0.17</b>
<b>Cellular Signaling</b>							
<b>BIN1</b>	NM_139343	<b>−5.16 ± 0.43</b>	−1.36 ± 0.32	−1.04 ± 0.16	1.34 ± 0.19	1.09 ± 0.11	1.06 ± 0.18
<b>CD2AP</b>	NM_012120	1.79 ± 0.31	1.21 ± 0.23	1.79 ± 0.18	1.21 ± 0.24	1.84 ± 0.06	1.19 ± 0.21
<b>PICALM</b>	NM_007166	<b>−5.62 ± 0.65</b>	1.05 ± 0.20	−1.4 ± 0.17	1.24 ± 0.19	1.13 ± 0.29	<b>−2.69 ± 0.17</b>
<b>Innate Immunity</b>							
<b>CR1</b>	NM_000573	−1.44 ± 0.16	<b>8.34 ± 0.81</b>	1.38 ± 0.42	1.33 ± 0.47	1.40 ± 0.15	<b>2.03 ± 0.19</b>
<b>CD33</b>	NM_001772	1.35 ± 0.32	1.05 ± 0.27	1.02 ± 0.22	1.09 ± 0.31	1.78 ± 0.07	1.71 ± 0.20
<b>Others</b>							
<b>MMP9</b>	NM_013599	<b>−17.2 ± 0.97</b>	<b>−2.91 ± 0.31</b>	−1.27 ± 0.14	−1.34 ± 0.21	1.48 ± 0.30	1.26 ± 0.31
<b>SORL1</b>	NM_003105	1.22 ± 0.06	1.36 ± 0.19	−1.18 ± 0.23	1.36 ± 0.28	−1.27 ± 0.34	−1.05 ± 0.23

<sup>a</sup> The results were normalized according to ACTB expression. <sup>b</sup> The values that differ significantly from control were highlighted in bold.

activity; however, when compared to their 4-methyl analogs with exactly the same substitution at C7, the 4-propyl analogs, *e.g.*, **9**, **13**, and **16** were much stronger inhibitors against both AChE or BChE; thus, it can be implied that C4 substitution with longer aliphatic moiety might enhance the inhibitory activity.

After determining the highest safe non-toxic concentration ( $\sim EC_{04-08}$ ) of the tested compounds on the SH-SY5Y cell lines, their effect on the expression level of fourteen genes known to be associated with AD was investigated. The changes in the expression level of these genes involved in beta-amyloid pathology, lipid metabolism, innate immunity and cellular signaling related to AD were investigated for compounds **16**, **13**, and **9**. As compared to the control cells, no significant change in the gene expression level after treatment with compound **13** at  $EC_{04}$  and  $EC_{08}$  was observed. This might indicate that compound **13** was not adequate for AD disease at the studied concentrations (Table 3).

AD is usually caused by rare and high rates of mutations in the amyloid beta precursor protein (APP), presenilin 1 (PSEN1), and apolipoprotein E (APOE). These genes alter the production of A $\beta$  peptide, in senile plaques.<sup>[23,24]</sup> A significant decrease in the expression of APP, PSEN1, and APOE genes, which are known as an essential risk factor for late-onset familial AD, was observed after treatment at  $EC_{04}$  of compound **16**. No significant difference was observed at  $EC_{08}$  dose of the compound **16**, as compared to the non-treated control.

In addition, we observed the inhibitory effect of compound **9** at  $EC_{08}$  on the PSEN1 and APOE gene expression. Although their metabolic roles are different, these genes have a common mechanism in AD development. Suppression of PSEN1 and APOE genes with the treatment of test compounds (**16** and **9**) in SH-SY5Y cells strongly suggests that it might inhibit the accumulation of A $\beta$ . In addition, a paradoxical effect was observed by the  $EC_{04}$  and  $EC_{08}$  of compound **16**. It has been previously reported that bidirectional and paradoxical reactions can occur entirely at appropriate doses or independently.<sup>[25]</sup>

Significant progress in the identification of genes that are associated with AD has recently been noticed. Genome-wide association studies (GWAS) are essential in identifying disease-associated genes in diseases with complex characteristics such as AD.<sup>[26]</sup> In these studies, changes were found in some genes such as Clusterin (CLU), Bridging Integrator 1 (BIN1) and the ATP-Binding Cassette Transporter A7 (ABCA7), which are also linked to cholesterol metabolism and

endocytosis.<sup>[27,28]</sup> Increased BIN1, CLU and ABCA7 expression levels were associated with APP accumulation.<sup>[29]</sup> We have detected a significant decrease in CLU, BIN1 and ABCA7 expression with the compound **16** treatment at the dose of  $EC_{04}$ . In addition, treatment at the  $EC_{08}$  dose of compound **9** resulted in a decrease in CLU expression. Thus, compounds **16** and **9** promote changes in levels of these genes' expression, favoring inhibition of the accumulation of A $\beta$ . These alterations in the expressions of BIN1, CLU and ABCA7 suggest that compounds **16** and **9** depict protective and therapeutic effects against AD pathogenesis.

It has been shown that complement receptor 1 (CR1) expression is processed differently in brain tissues, leading to disparity at functional molecule levels, being a crucial factor for A $\beta$  plaque clearance.<sup>[30]</sup> Similarly, another study has reported that increased CR1 expression may be protective due to the increased number of CR1 molecules available to clear A $\beta$  plaques.<sup>[31]</sup> This study has also documented an increase in CR1 expression level with both compounds **16** (at  $EC_{04}$  dose) and **9** (at  $EC_{08}$  dose) treatment SH-SY5Y cells. These findings may further support the protective and therapeutic effect of these compounds against AD.

One of the genes identified as one of the susceptibility loci for late-onset AD in GWAS is the phosphatidylinositol binding clathrin assembly protein (PICALM).<sup>[27]</sup> PICALM is an adapter protein that modulates brain A $\beta$  pathology and tau accumulation and plays critical roles in clathrin-mediated endocytosis and autophagy.<sup>[32]</sup> It has been shown that the reduction of PICALM expression has significant effects on the processing of APP, which may be beneficial for slowing or preventing the development of AD *via* reducing endocytosis and secretase activity.<sup>[33]</sup> The decrease in PICALM expression level observed in the present study after treatment with compounds **16** and **9** may further indicate that they are essential in slowing the development of AD. Matrix metalloproteinases (MMP) are other genes thought to play a role in the pathophysiology of AD disease.<sup>[34]</sup> MMP-9 are associated with immunological and cardiovascular diseases, cancer, and pathological processes affecting the central nervous system.<sup>[35–38]</sup> In recent studies, MMP-9 has been shown to play a role in the physiological catabolism of A $\beta$ .<sup>[39]</sup> The strong inhibitions observed in the expression of MMP-9 with compound **16** could be accepted as induction of immune responses in such a way to increase brain resistance to amyloid accumulation.

## Conclusions

The current study investigated the ChE inhibitory capacity of a series of synthetic coumarins, along with the *in vitro* transcriptional effects that might be further considered in the treatment of AD. Since none of the drugs currently used in AD treatment can provide a complete cure, it is crucial to find new therapeutic drugs. Three strongest ChEs inhibitors (**9**, **13**, and **16**) displayed proper interactions in the amino acid residues located in the active gorge of both AChE and BChE. In conclusion, the results presented in this study strongly support two compounds, namely 7-hydroxy-4-propyl-coumarin (**9**) and 7-ethoxy-4-propyl-2H-chromen-2-one (**16**), as the most effective coumarin derivatives for further studies for AD therapy.

## Experimental Section

### Microtiter Assays for ChE Inhibition

AChE and BChE inhibitory activities of the previously synthesized compounds<sup>[17]</sup> were determined by the slightly modified spectrophotometric method developed by Ellman et al.<sup>[40]</sup> Briefly, 140  $\mu$ L of sodium phosphate buffer (pH 8.0), 10  $\mu$ L of DTNB (5,5-dithio-bis-2-nitrobenzoic acid), 20  $\mu$ L of the test solution and 20  $\mu$ L of AChE/BChE solution were added by multi-channel automatic pipette (Gilson pipetman, France) in a 96-well microplate and incubated for 10 min at 25 °C. The reaction was then initiated by addition of 10  $\mu$ L of acetylthiocholine iodide/butyrylthiocholine chloride. Hydrolysis of acetylthiocholine iodide/butyrylthiocholine chloride was monitored by the formation of the yellow 5-thio-2-nitrobenzoate anion as a result of the reaction of DTNB with thiocholines which was catalyzed by the enzymes. Galantamine hydrobromide was used as the reference drug.

The enzyme inhibition assays were carried out using a 96-well microplate reader (VersaMax Molecular Devices, USA). The measurements and calculations were evaluated by using Softmax PRO 4.3.2.LS software. The inhibition percentage of AChE and BChE was determined by comparison of the reaction rates of samples vs. blank sample using the formula  $I\% = 100 - [(A_1/A_2) \times 100]$ , where  $A_1$  is the absorbance of the sample solutions at 412 nm and  $A_2$  is the average absorbance of the control solutions at the same wavelength. The results are given as mean  $\pm$  standard deviation (S.D.) of the % inhibitions obtained from three parallel experiments. Selectivity index (SI) values, also known

as AChE selectivity index of the compounds, which had IC<sub>50</sub> values against both enzymes, were calculated through IC<sub>50</sub> BChE/IC<sub>50</sub> AChE affinity ratio.

### Molecular Docking Experiments

Crystal structures of AChE and BChE were retrieved from the protein data bank (PDB) with the IDs of 4M0E<sup>[41]</sup> and 4TPK<sup>[42]</sup> respectively. Extra water and co-factor molecules were removed from the systems and the dimensions of the co-crystal ligands were used to detect the ligand-binding domains for the docking simulations.<sup>[43]</sup> A single chain was selected for each protein and the missing side-chain and backbone atoms were added using the protein preparation wizard of Maestro,<sup>[44]</sup> and the total energies of the systems were minimized to remove any possible clashes between the atoms. The ionization of the systems was set to a biological pH. Chemical structures of the ligands were sketch in Maestro and their 3D structures were generated in the LigPrep module of Maestro.<sup>[45]</sup> The default parameters, ionizer, and OPLS3 force field were used for the calculations.

### Cell Culture Experiments

#### Cell Culture

SH-SY5Y, a human neuroblastoma cell line, was cultured in Dulbecco's Modified Eagle Medium/Nutrient Mixture F-12 (DMEM/F-12) supplemented with 10% heat-inactivated fetal bovine serum (FBS) and 1% antibiotics. Cells were incubated at 37 °C with 5% CO<sub>2</sub> in a humidified atmosphere.

#### Cell Viability Assay

SH-SY5Y cells were seeded at an initial density of  $5 \times 10^3$  cells/well in 96-well plates and allowed to attach overnight in DMEM/F12 medium with necessary supplementation. The cells were treated with solvent (DMSO), as a control, and varying concentrations of test compounds (**1-16**). Then, the cells were incubated in humidified 5% CO<sub>2</sub> atmosphere at 37 °C. After 24 h incubation, the medium was discarded and 0.5% crystal-violet (w/v; in 50% methanol) solution was added. Plates were incubated for 10 min at room temperature, washed with water and adsorbed dye was eluted out with Na-citrate (0.1 M Na-citrate in 50% ethanol, pH 4.2). The absorbance was measured at a wavelength of 600 nm which was proportional to cell viability. Net absorbance (blank subtracted) was

used to calculate the percentage of cell viability with respect to control (untreated cells).<sup>[46]</sup>

### RNA Isolation and Real-Time RT-PCR

Total RNA was isolated from the control and treated cells using RNeasy Plus Universal Mini Kit (Qiagen) according to the manufacturer instructions with slight modifications. RNA concentration was determined using Nanodrop (MaestroNano Micro-volume Spectrophotometer, USA) and total RNA (1 µg) was used in reverse-transcription (RT) reactions, using Easy Script cDNA Synthesis Kit (ABM). Gene expression was analyzed by Exicycler 96 Thermal Block from Bioneer (Korea) with KiloGreen 2X qPCR Master Mix (ABM, Canada) using gene-specific primers. The gene-specific primer sequences are shown in Table 5. Changes in mRNA expression of the different genes were normalized with β-actin. The relative expressions at the mRNA level were quantified by the  $2^{-\Delta\Delta Ct}$  method.<sup>[47]</sup>

### Statistical Analysis

Statistical calculations were performed using the Minitab 13 statistical software bundle (Minitab, Inc., State College, PA, USA). The results were expressed as means, including their standard error of means (SEM). Student's *t*-test was applied and \**P* < 0.05 was chosen as the level of statistical significance.

### Abbreviations

ABCA7 ATP-Binding Cassette Transporter A7; ACh acetylcholine; AChE acetylcholinesterase; AD Alzheimer's disease; APOE apolipoprotein E; APP amyloid

beta precursor protein; BChE butyrylcholinesterase; BIN1 Bridging Integrator 1; ChE cholinesterase; CLU clusterin; CR1 complement receptor 1; DMEM/F-12 Dulbecco's Modified Eagle Medium/Nutrient Mixture F-12; DMSO dimethyl sulfoxide; DTNB 5,5-dithiobis(2-nitrobenzoic acid); FBS fetal bovine serum; GWAS genome-wide association studies; IR infrared spectroscopy; NMDA *N*-methyl-D-aspartate; NMR nuclear magnetic resonance spectroscopy; MMP Matrix metalloproteinases; PDB protein data bank; PICALM phosphatidylinositol binding clathrin assembly protein; PSEN1 presenilin 1; SEM standard error of means.

### Acknowledgements

Cell culture studies were supported by Scientific Research Project Funds provided through Pamukkale University (Denizli, Turkey) with the project No: 2019FEBE021. The work was supported by Medical University of Lublin DS28 (Poland).

### Conflict of Interest

The authors declare no conflict of interest.

### Data Availability Statement

The data that support the findings of this study are available from the corresponding author upon reasonable request.

**Table 5.** Gene-specific primer sequences.

Gene Name	Forward Sequence	Reverse Sequence	TM
ACTB	GCCGCCAGCTCACCAT	GATGCCTCTCTGCTCTGGG	59.00
APP	GCCCTGCGGAATTGACAAG	CCATCTGCATAGTCTGTGTCTG	62.00
MMP9	GGGACGCAGACATCGTCATC	TCGTCATCGTCGAAATGGGC	62.00
PSEN1	GCAGTATCCTCGCTGGTGAAGA	CAGGCTATGGTTGTGTTCCAGTC	54.50
APOE	GGGTGCGTTTTGGGATTACCTG	CAACTCCTTCATGGTCTCGTCC	54.50
CLU	TGCGGATGAAGGACCAGTGTGA	TTTCTGGTCAACCTCTCAGCG	54.50
CR1	TAGGTGTCAGCCTGGCTTTGTC	GACATCTGGAGGTGGCTGACAT	54.50
PICALM	GGCAGCATTAGAGGAAGAACAGG	CTGCTGAGGTGGATACAGGAGA	54.50
BIN1	CGTCAACACGTTCCAGAGCATC	CTTGACCGTGAAGGTGTTGCTC	54.50
ABCA7	CACTCTCCGAGAGCTAGACAC	CTCCATATCTGTGTCCGACGA	54.50
CD33	GTGACTACGGAGAGAACCATCC	GCTGTAACACCAGCTCCTCCAA	54.50
CD2AP	CAAAGCCTGAACTGATAGCTGC	GGACTTGTGGAGCTGCTGGTTT	54.50
SORL1	GAACACCTGTCTTCGCAACCAG	TGTCCAGGTCACAGATGGTGGT	54.50

## Author Contribution Statement

IEO – Conceptualization; Methodology; Resources; FSSD – Investigation; Validation; RES – Software; Formal analysis; Methodology; Writing; SI – Investigation; OOA – Investigation; Writing – Original Draft; GCT – Writing - Review & Editing; AS – Conceptualization; Methodology; Resources; AMZ – Methodology; Resources; SVL – Conceptualization; Writing – Review & Editing; Visualization; AS – Writing – Review & Editing; Visualization; KSW – Conceptualization; Methodology; Writing - Review & Editing; Project administration; GT – Conceptualization; Methodology; Resources.

## References

- [1] P. Scheltens *et al.* 'Alzheimer's disease,' *Lancet* (London, England) **2021**, 397, 1577–1590.
- [2] M. S. Uddin, M. T. Kabir, T. Behl, and G. M. Ashraf, 'Reconsidering and Reforming the Amyloid Cascade Hypothesis', *Curr. Protein Pept. Sci* **2021**, 22, 449–457.
- [3] H. Hampel *et al.* 'Revisiting the Cholinergic Hypothesis in Alzheimer's Disease: Emerging Evidence from Translational and Clinical Research,' *J. Prev. Alzheimer's Dis.* **2019**, 6, 2–15.
- [4] M. Saxena and R. Dubey, 'Target Enzyme in Alzheimer's Disease: Acetylcholinesterase Inhibitors', *Curr. Top. Med. Chem.* **2019**, 19, 264–275.
- [5] S. Darvesh, 'Butyrylcholinesterase as a Diagnostic and Therapeutic Target for Alzheimer's Disease.' *Curr. Alzheimer Res.* **2016**, 13, 1173–1177.
- [6] A. Misrani, S. Tabassum, and L. Yang, 'Mitochondrial Dysfunction and Oxidative Stress in Alzheimer's Disease', *Front. Aging Neurosci.* **2021**, 13, 617588.
- [7] D. J. R. Lane, B. Metselaar, M. Greenough, A. I. Bush, and S. J. Ayton, 'Ferroptosis and NRF2: an emerging battlefield in the neurodegeneration of Alzheimer's disease', *Essays Biochem.* **2021**, 65, 925–940.
- [8] S. Matsunaga, H. Fujishiro, and H. Takechi, 'Efficacy and Safety of Cholinesterase Inhibitors for Mild Cognitive Impairment: A Systematic Review and Meta-Analysis', *J. Alzheimers. Dis.* **2019**, 71, 513–523.
- [9] I. E. Orhan and H. O. Gulcan, 'Coumarins: Auspicious Cholinesterase and Monoamine Oxidase Inhibitors', *Curr. Top. Med. Chem.* **2015**, 15, 1673–1682.
- [10] L. G. de Souza, M. N. Rennã, and J. D. Figueroa-Villar, 'Coumarins as cholinesterase inhibitors: A review', *Chem. Biol. Interact.* **2016**, 254, 11–23.
- [11] L. Pisani, M. Catto, A. De Palma, R. Farina, S. Cellamare, and C. D. Altomare, 'Discovery of Potent Dual Binding Site Acetylcholinesterase Inhibitors via Homo- and Heterodimerization of Coumarin-Based Moieties', *ChemMedChem* **2017**, 12, 1349–1358.
- [12] S. Montanari *et al.* 'Multitarget Strategy to Address Alzheimer's Disease: Design, Synthesis, Biological Evaluation, and Computational Studies of Coumarin-Based Derivatives', *ChemMedChem* **2016**, 11, 1296–1308.
- [13] F. S. Senol, K. Skalicka Wozniak, M. T. H. Khan, I. Erdogan Orhan, B. Sener, and K. Głowniak, 'An in vitro and in silico approach to cholinesterase inhibitory and antioxidant effects of the methanol extract, furanocoumarin fraction, and major coumarins of *Angelica officinalis* L. fruits', *Phytochem. Lett.* **2011**, 4, 462–467.
- [14] I. E. Orhan, F. S. Senol, S. Shekfeh, K. Skalicka-Wozniak, and E. Banoglu, 'Pteryxin - A promising butyrylcholinesterase-inhibiting coumarin derivative from *Mutellina purpurea*', *Food Chem. Toxicol.* **2017**.
- [15] I. E. Orhan *et al.*, 'Combined molecular modeling and cholinesterase inhibition studies on some natural and semisynthetic O-alkylcoumarin derivatives', *Bioorg. Chem.* **2019**, 84, 355–362.
- [16] I. E. Orhan *et al.*, 'Profiling Auspicious Butyrylcholinesterase Inhibitory Activity of Two Herbal Molecules: Hyperforin and Hyuganin C', *Chem. Biodiversity* **2019**.
- [17] G. Tătăringă, C. Tuchiluş, A. Jităreanu, and A. Zbancioc, 'Antimicrobial prospection of some coumarin derivatives', *Farmacia* **2018**, 66, 323–330.
- [18] C. Patterson, 'World Alzheimer report 2018', **2018**.
- [19] D. Kang *et al.*, 'Discovery, optimization, and target identification of novel coumarin derivatives as HIV-1 reverse transcriptase-associated ribonuclease H inhibitors', *Eur. J. Med. Chem.* **2021**, 225, 113769.
- [20] L. Lei *et al.*, 'Coumarin derivatives from *Ainsliaea fragrans* and their anticoagulant activity', *Sci. Rep.* **2015**, 5, 13544.
- [21] S. H. Emam, A. Sonousi, E. O. Osman, D. Hwang, G.-D. Kim, and R. A. Hassan, 'Design and synthesis of methoxyphenyl- and coumarin-based chalcone derivatives as anti-inflammatory agents by inhibition of NO production and down-regulation of NF- $\kappa$ B in LPS-induced RAW264.7 macrophage cells', *Bioorg. Chem.* **2021**, 107, 104630.
- [22] A. Uttarkar, A. P. Kishore, S. M. Srinivas, S. Rangappa, R. Kusanur, and V. Niranjan, 'Coumarin derivative as a potent drug candidate against triple negative breast cancer targeting the frizzled receptor of wntless-related integration site signaling pathway.' *J. Biomol. Struct. Dyn.* **2022**, 1–13.
- [23] P. H. St George-Hyslop and A. Petit, 'Molecular biology and genetics of Alzheimer's disease', *C. R. Biol.* **2005**, 328, 119–130.
- [24] J. Tcw and A. M. Goate, 'Genetics of  $\beta$ -Amyloid Precursor Protein in Alzheimer's Disease', *Cold Spring Harb. Perspect. Med.* **2017**, 7.
- [25] S. W. Smith, M. Hauben, and J. K. Aronson, 'Paradoxical and bidirectional drug effects.', *Drug Saf.* **2012**, 35, 173–189.
- [26] A. C. Need and D. B. Goldstein, 'Whole genome association studies in complex diseases: where do we stand?', *Dialogues Clin. Neurosci.* **2010**, 12, 37–46.
- [27] G. Tosto and C. Reitz, 'Genome-wide association studies in Alzheimer's disease: a review', *Curr. Neurol. Neurosci. Rep.* **2013**, 13, 381.
- [28] P. Dourlen, D. Kilinc, N. Malmanche, J. Chapuis, and J.-C. Lambert, 'The new genetic landscape of Alzheimer's disease: from amyloid cascade to genetically driven synaptic failure hypothesis?', *Acta Neuropathol.* **2019**, 138, 221–236.

- [29] C. M. Karch, A. T. Jeng, P. Nowotny, J. Cady, C. Cruchaga, and A. M. Goate, 'Expression of novel Alzheimer's disease risk genes in control and Alzheimer's disease brains,' *PLoS One*, **2012**, *7*, e50976.
- [30] L.-N. Hazrati *et al.*, 'Genetic association of CR1 with Alzheimer's disease: a tentative disease mechanism,' *Neurobiol. Aging* **2012**, *33*, 2949.e5-2949.e12.
- [31] G. C. Kretschmar *et al.*, 'First Report of CR1 Polymorphisms and Soluble CR1 Levels Associated with Late Onset Alzheimer's Disease (LOAD) in Latin America,' *J. Mol. Neurosci.* **2020**, *70*, 1338–1344.
- [32] K. Ando *et al.*, 'Picalm reduction exacerbates tau pathology in a murine tauopathy model,' *Acta Neuropathol.* **2020**, *139*, 773–789.
- [33] R. S. Thomas, A. Henson, A. Gerrish, L. Jones, J. Williams, and E. J. Kidd, 'Decreasing the expression of PICALM reduces endocytosis and the activity of  $\beta$ -secretase: implications for Alzheimer's disease,' *BMC Neurosci.* **2016**, *17*, 50.
- [34] M. Brkic, S. Balusu, C. Libert, and R. E. Vandenbroucke, 'Friends or Foes: Matrix Metalloproteinases and Their Multifaceted Roles in Neurodegenerative Diseases,' *Mediators Inflamm.* **2015**, *2015*, 620581.
- [35] M. Ram, Y. Sherer, and Y. Shoenfeld, 'Matrix metalloproteinase-9 and autoimmune diseases,' *J. Clin. Immunol.* **2006**, *26*, 299–307.
- [36] P. Liu, M. Sun, and S. Sader, 'Matrix metalloproteinases in cardiovascular disease,' *Can. J. Cardiol.* **2006**, *22*, 25B-30B.
- [37] S. M. Reinhard, K. Razak, and I. M. Ethell, 'A delicate balance: role of MMP-9 in brain development and pathophysiology of neurodevelopmental disorders,' *Front. Cell. Neurosci.* **2015**, *9*, 280.
- [38] A. Beroun, S. Mitra, P. Michaluk, B. Pijet, M. Stefaniuk, and L. Kaczmarek, 'MMPs in learning and memory and neuropsychiatric disorders,' *Cell. Mol. Life Sci.* **2019**, *76*, 3207–3228.
- [39] S. Lorenzl *et al.*, 'Increased plasma levels of matrix metalloproteinase-9 in patients with Alzheimer's disease,' *Neurochem. Int.* **2003**, *43*, 191–196.
- [40] G. L. Ellman, K. D. Courtney, V. J. Andres, and R. M. Feather-Stone, 'A new and rapid colorimetric determination of acetylcholinesterase activity,' *Biochem. Pharmacol.* **1961**, *7*, 88–95.
- [41] J. Cheung, E. N. Gary, K. Shiomi, and T. L. Rosenberry, 'Structures of human acetylcholinesterase bound to dihydrodantoinone I and territrem B show peripheral site flexibility,' *ACS Med. Chem. Lett.* **2013**, *4*, 1091–1096.
- [42] B. Brus *et al.*, 'Discovery, biological evaluation, and crystal structure of a novel nanomolar selective butyrylcholinesterase inhibitor,' *J. Med. Chem.* **2014**, *57*, 8167–8179.
- [43] R. A. Friesner *et al.*, 'Extra precision glide: docking and scoring incorporating a model of hydrophobic enclosure for protein-ligand complexes,' *J. Med. Chem.* **2006**, *49*, 6177–6196.
- [44] G. M. Sastry, M. Adzhigirey, T. Day, R. Annabhimoju, and W. Sherman, 'Protein and ligand preparation: parameters, protocols, and influence on virtual screening enrichments,' *J. Comput. Aided. Mol. Des.* **2013**, *27*, 221–234.
- [45] J. R. Greenwood, D. Calkins, A. P. Sullivan, and J. C. Shelley, 'Towards the comprehensive, rapid, and accurate prediction of the favorable tautomeric states of drug-like molecules in aqueous solution,' *J. Comput. Aided. Mol. Des.* **2010**, *24*, 591–604.
- [46] G. Ç. Turgut *et al.*, 'Computer design, synthesis, and bioactivity analyses of drugs like fingolimod used in the treatment of multiple sclerosis,' *Bioorg. Med. Chem.* **2017**, *25*, 483–495.
- [47] S. Yavuz *et al.*, 'Synthesis and Functional Investigations of Computer Designed Novel Cladribine-Like Compounds for the Treatment of Multiple Sclerosis,' *Arch. Pharm. (Weinheim)*. **2017**, 350.

Received April 4, 2022  
Accepted October 19, 2022